Mutant Cholinesterases Possessing Enhanced Capacity for Reactivation of Their Phosphonylated Conjugates†

Zrinka Kovarik,‡,§ Zoran Radić,‡ Harvey A. Berman,|| Vera Simeon-Rudolf,§ Elsa Reiner,§ and Palmer Taylor*,‡

Department of Pharmacology, University of California at San Diego, La Jolla, California 92093-0636, Institute for Medical Research and Occupational Health, HR-10000 Zagreb, Croatia, and Department of Pharmacology and Toxicology, School of Medicine, University at Buffalo, Buffalo, New York 14214

Received December 5, 2003; Revised Manuscript Received January 12, 2004

ABSTRACT: Selective mutants of mouse acetylcholinesterase (AChE; EC 3.1.1.7) phosphonylated with chiral S_P- and R_P-cycloheptyl, -3,3-dimethylbutyl, and -isopropyl methylphosphonyl thiocholines were subjected to reactivation by the oximes HI-6 and 2-PAM and their reactivation kinetics compared with wild-type AChE and butyrylcholinesterase (EC 3.1.1.8). Mutations in the choline binding site (Y337A, Y337A/F338A) or combined with acyl pocket mutations (F295L/Y337A, F297I/Y337A, F295L/F297I/Y337A) were employed to enlarge active center gorge dimensions. HI-6 was more efficient than 2-PAM (up to 29000 times) as a reactivator of S_P-phosphonates (k_r ranged from 50 to 13000 min^{-1} M^{-1}), while R_P conjugates were reactivated by both oximes at similar, but far slower, rates (k_r < 10 min^{-1} M^{-1}). The Y337A substitution accelerated all reactivation rates over the wild-type AChE and enabled reactivation even of R_P-cycloheptyl and R_P-3,3-dimethylbutyl conjugates that when formed in wild-type AChE are resistant to reactivation. When combined with the F295L or F297I mutations in the acyl pocket, the Y337A mutation showed substantial enhancements of reactivation rates of the S_P conjugates. The greatest enhancement of 120-fold was achieved with HI-6 for the F295L/Y337A phosphonylated with the most bulky alkoxy moiety, S_P-cycloheptyl methylphosphonate. This significant enhancement is likely a direct consequence of simultaneously increasing the dimensions of both the choline binding site and the acyl pocket. The increase in dimensions allows for optimizing the angle of oxime attack in the spatially impacted gorge as suggested from molecular modeling. Rates of reactivation reach values sufficient for consideration of mixtures of a mutant enzyme and an oxime as a scavenging strategy in protection and treatment of organophosphate exposure.

Organophosphates are potent inhibitors of acetylcholinesterase (AChE;[1] EC 3.1.1.7) and butyrylcholinesterase (BChE; EC 3.1.1.8). The progressive inhibition of cholinesterases by organophosphates is due to phosphylation (denotes phosphonylation and phosphorylation) of their active center serine characterized by the formation of conjugates, which react very slowly with water. Inhibition of AChE is the main cause of organophosphate toxicity (*1*). Early studies on reactivation of the enzyme by Wilson and colleagues showed that, by directing nucleophiles to the active site, conjugated organophosphates could be released, regenerating the active enzyme (*2*, *3*). Strong nucleophiles such as oximes are particularly effective in reactivating organophosphate−cholinesterase conjugates. Nucleophilic strength, the orientation of the nucleophile with respect to the conjugated organophosphate, and the rate of aging (postinhibitory dealkylation) are three factors well-known to affect reactivation. During the past several decades, effective oximes have been developed as antidotes to cholinesterase poisoning that greatly improve efficacy of treatment of acute organophosphate poisoning (*4*). The monopyridinium oxime, 2-PAM, and bispyridinium oxime, HI-6, are the most potent reactivating agents in use in antidotal therapy (Figure 1). The effectiveness of oxime reactivators is primarily attributed to the nucleophilic displacement rate of the organophosphates, but efficiency varies with the structure of the bound organophosphate, the source of enzyme and the oxime.

The crystal structures of AChE (*5*−*7*) provide templates for detailed structural studies on ligand access to the impacted enzyme active center gorge and steric constraints within the active center gorge that govern selectivity in organophosphate inhibition (*8*−*13*) and oxime reactivation (*14*−*18*). The site of conjugation by organophosphates lies at the base of a narrow and 18−20 Å deep gorge. The gorge wall of AChE is lined largely by aromatic side chains contributing to a well-defined acyl pocket and choline binding site at the base of the gorge (*19*, *20*). Therefore, the orientation of the associated

† This work was supported by Grants DAMD17C8014 and R37-GM18360 to P.T., Grant 0022014 to V.S.-R., and fellowships of the Ministry of Science and Technology of the Republic of Croatia and the Wood-Whelan Research Fellowship (IUBMB) to Z.K.

* To whom correspondence should be addressed. Telephone: 858-534-1366. Fax: 858-534-8248. E-mail: pwtaylor@ucsd.edu.

‡ University of California at San Diego.

§ Institute for Medical Research and Occupational Health.

|| University at Buffalo.

[1] Abbreviations: AChE, acetylcholinesterase; ATCh, acetylthiocholine iodide; BChE, butyrylcholinesterase; 2-PAM, 2-(hydroxyiminomethyl)-1-methylpyridinium iodide; HI-6, 1-(2′-hydroxyiminomethyl-1′-pyridinium)-3-(4″-carbamoyl-1″-pyridinium)-2-oxapropane dichloride.

10.1021/bi036191a CCC: $27.50
Published on Web 02/26/2004

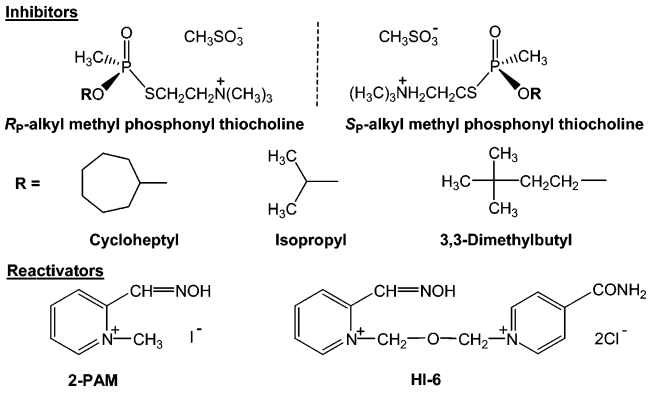

FIGURE 1: Structures of the organophosphonates and oximes used in this study.

and conjugated ligands within narrow confines of the gorge and the rates of nucleophilic attack by oxime at the conjugated phosphorus atom become important determinants of the reactivation mechanism.

In this study, we investigated structural and kinetic bases for reactivation of the enzyme conjugates by oximes using a combined structure−activity approach where both inhibitor and enzyme were modified systematically. Mouse AChE was modified within the choline binding site (Y337A, F338A) and the acyl pocket (F295L, F297I) in various mutation permutations. The mutant AChE species, except for F338A, contained mutations that resemble residues found at structurally equivalent positions in BChE (residue numbering corresponds to mouse AChE). This enabled us to examine the basis of the divergence between oxime reactivation of phosphonylated AChE and BChE. By using a congeneric series of S_P and R_P enantiomeric pairs of alkyl methylphosphonates and two related oximes of different dimensions, HI-6 and 2-PAM (Figure 1), subtle differences in reactivation capability have been analyzed with the objective of enhancing reactivation rates.

MATERIALS AND METHODS

Chemicals. S_P- and R_P-alkyl methylphosphonyl thiocholines were synthesized and isolated as resolved S_P and R_P enantiomers (*8*). Stock solutions in acetonitrile were kept at −20 °C, and aliquots were diluted in water immediately before use. HI-6 was a gift of B. P. Doctor at Walter Reed Army Research Center, Washington, DC. 2-PAM, acetylthiocholine iodide (ATCh), 5,5′-dithiobis(2-nitrobenzoic acid), and bovine serum albumin (BSA) were purchased from Sigma Chemical Co., St. Louis, MO. Both oximes, HI-6 and 2-PAM, were kept at −20 °C, and they were dissolved and diluted in water immediately before use.

Enzymes. Preparation, expression, purification, and characterization of recombinant wild-type mouse AChE and wild-type mouse BChE and AChE mutants were described in detail in previous studies (*9*, *13*, *19*, *21*).

Oxime Reactivation of the Phosphonylated Enzyme. Wild-type and mutant enzymes (concentrations between 0.01 and 1.0 μM) were reacted with an ∼10% molar excess of the corresponding alkyl methylphosphonate until inhibition was greater than 90%. Typical inhibition times were 30 min to 2 h, except for the case of slower inhibition with R_P enantiomers, when the required time was up to 6 h. The inhibited enzyme was passed through a Sephadex G-50 spin column (Pharmacia) to remove excess unconjugated organophosphate and incubated with specified concentrations of oxime in 10 mM Tris-HCl buffer, pH 8.0, containing 0.01% BSA, 40 mM $MgCl_2$, and 100 mM NaCl. At specified time intervals, 5−10 μL of the reactivation mixture was diluted up to 100-fold, and residual activity was measured at 22 °C by the Ellman method using ATCh as substrate (1.0 mM final concentration) (*22*). An equivalent sample of uninhibited enzyme was passed through a parallel column, diluted to the same extent as the inhibition mixture, and control activity was measured in the presence of oxime at concentrations used for reactivation. Both activities of the control and reactivation mixture were corrected for oxime-induced hydrolysis of ATCh, whenever oxime concentrations were greater than 1.0 mM.

Scheme 1

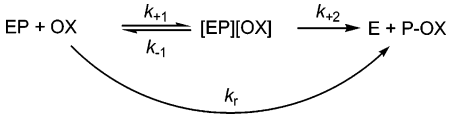

Kinetics of Oxime Reactivation. Oxime reactivation of phosphylated cholinesterases proceeds according to Scheme 1. In this scheme EP is the phosphylated enzyme, [EP][OX] is the reversible Michaelis-type complex between EP and the oxime (OX), E is the active enzyme and P−OX the phosphonylated oxime, k_{+2} is the maximum first-order rate constant, and k_r is the overall second-order rate constant of reactivation.

Scheme 1 is defined by the equation:

$$\ln\frac{[EP]_0}{[EP]_t} = \frac{k_{+2}[OX]}{K_{OX} + [OX]}\, t = k_{obs}t \qquad (1)$$

where $[EP]_0$ and $[EP]_t$ are the concentrations of the phosphonylated enzyme at time zero and at time t, respectively. K_{ox} is equal to the ratio $(k_{-1} + k_{+2})/k_{+1}$, and it typically approximates the dissociation constant of the [EP][OX] complex. k_{obs} is the observed first-order rate constant of reactivation at any given oxime concentration.

When $K_{ox} \gg [OX]$, eq 1 simplifies to

$$\ln\frac{[EP]_0}{[EP]_t} = \frac{k_{+2}}{K_{OX}}[OX]t = k_r[OX]t = k_{obs}t \qquad (2)$$

where from it follows that

$$k_r = \frac{k_{+2}}{K_{OX}} \qquad (3)$$

Experimental data were presented as percent of reactivation

$$\%\ \text{reactivation} = \frac{v_{(EP+OX)_t}}{v_{(E+OX)}} \times 100 \qquad (4)$$

where $v_{(EP+OX)_t}$ denotes the activity of the reactivated enzyme at time t and $v_{(E+OX)}$ stands for the activity of the unmodified enzyme incubated with oxime. Both activities were corrected for oxime-induced hydrolysis of ATCh. If the enzyme was not completely inhibited prior to reactivation, both activities in eq 4 were also corrected for the enzyme activity at time

zero. Since (100 − % reactivation) is equal to $100[EP]_t / [EP]_0$, one can relate the experimental data to eqs 1 and 2.

At each oxime concentration, k_{obs} was calculated from the slope of the initial portion of log(100 − % reactivation) vs time of reactivation plot as $k_{obs} = -2.303 \times$ slope, assuming an approach to 100% reactivation. When reactivation followed eq 1, k_{+2} and K_{ox} were obtained by the nonlinear fit of the relationship between k_{obs} vs [OX]; k_r was calculated from eq 3. When reactivation followed eq 2, k_{obs} vs [OX] was linear, and the slope corresponded to k_r; in this case constants k_{+2} and K_{ox} could not be determined.

Molecular Modeling. Molecular modeling analysis was performed in order to ascertain probable HI-6 orientations inside the active center gorges of S_P-cycloheptyl methylphosphonylated wild-type mouse AChE and F295L/Y337A mouse AChE, where the HI-6 oxime group was facing the phosphorus conjugated to the AChE active center serine. The model of HI-6 was built as described earlier (*14*, *18*) and docked manually inside active center gorges of either S_P-cycloheptyl wild-type mouse AChE (taken from ref *18*) or S_P-cycloheptyl F295L/Y337A mutant mouse AChE (generated from phosphonylated wild-type mouse AChE using the Insight II program suite, Accelrys, San Diego) to achieve starting structures of the complex. Molecular dynamics of the complex was then performed using the procedure described earlier (*14*) and repeated 20 times for both wild-type and mutant complexes. During the computation the conformation of the HI-6 molecule was unrestricted, as were the side chains of AChE residues at positions 295, 297, 338, and phosphonylated serine at 203. The resulting 20 conformers of the complex were analyzed for their total energy and distance between the oxime group oxygen and phosphonate phosphorus.

RESULTS

Oxime Reactivation Kinetics. Recombinant DNA-expressed mouse cholinesterases phosphonylated with S_P- and R_P-alkyl methylphosphonyl thiocholines were subjected to reactivation by HI-6 and 2-PAM. The series of reactivation reactions were run over a wide concentration range of oximes to determine constants k_{+2}, K_{ox}, and k_r (Figure 2). The results for the 74 distinct oxime−enzyme combinations are listed in Tables 1−6. In 18 reactions, the rates of reactivation were so slow that rate constants could not be reliably determined. For these reactions only the maximum percent of reactivation obtained within the stated time is listed in the tables. For reactivation of the triple mutant F295L/F297I/Y337A only limiting values of constants were calculated because reactivation was measured at one oxime concentration only. For 8 reactions the k_{obs} values were a linear function of the oxime concentration; consequently, only the bimolecular k_r constants could be calculated. For 44 reactions, all three constants (k_{+2}, K_{ox}, k_r) were obtained as presented in Figure 2 and are displayed in the tables including the maximum percent of reactivation obtained with the highest oxime concentration after the indicated time of reaction. The mean relative standard error of k_{+2} was 11%, while the corresponding errors of K_{ox} and k_r were larger, 43% and 39%, respectively.

All k_{obs} constants were calculated from the initial slope of the reactivation profile. For some of the reactions, typically those where the reactivation was not complete (cf. Tables 1−6), the kinetics at the longer time intervals deviated from the first-order process described in eqs 1 and 2. This deviation could be due to a fraction of the phosphonylated enzyme aging with the loss of the alkoxy group, reinhibition of the active enzyme by the phosphonylated oxime, the presence of a minor abundance oxime-resistant conformation, and/or spontaneous reactivation of the phosphonylated conjugates.

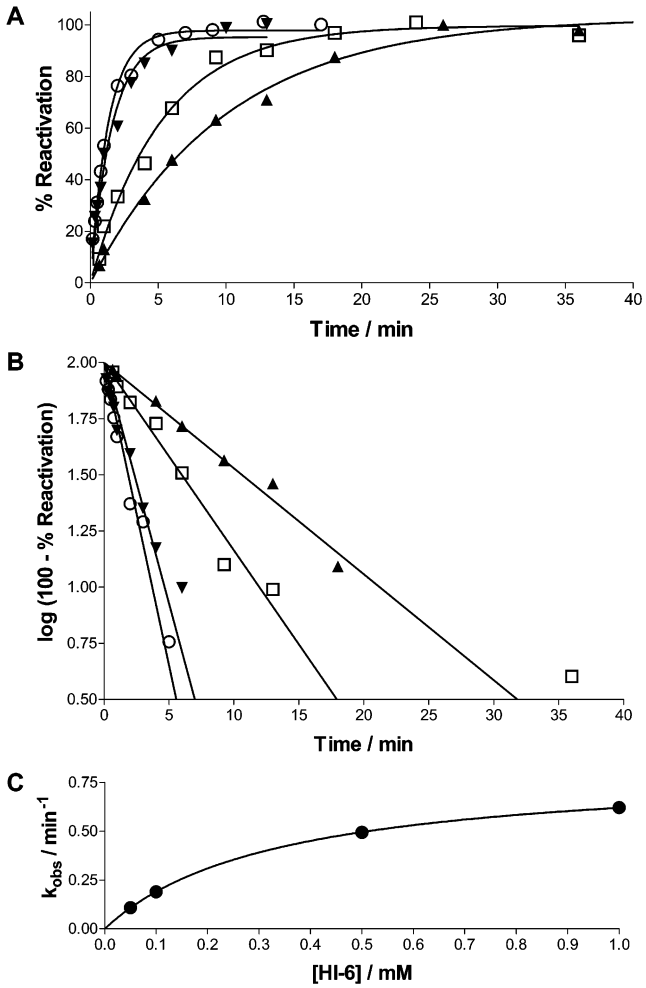

FIGURE 2: Reactivation of the S_P-isopropyl methylphosphonyl F297I/Y337A conjugate by HI-6. (A) Single datum points indicate calculated percent reactivation by eq 4 after the designated time of reactivation with (○) 1, (▼) 0.5, (□) 0.1, and (▲) 0.05 mM HI-6. (B) Slopes of the reactivation curve yield k_{obs} constants. (C) k_{obs} is plotted as a function of HI-6 and the line fitted using eq 1.

Aging of the three S_P-phosphonate-conjugated Y337A mutants was examined by measuring the extent of reactivation with high HI-6 concentrations added at designated intervals after inhibition with the phosphonate and removal of excess inhibitor. Aging of S_P-isopropyl and S_P-3,3-dimethylbutyl methylphosphonyl Y337A conjugates was not detected over 36 h, while the aging rate constant of S_P-cycloheptyl methyl conjugated Y337A was 0.005 min^{-1}. This is faster than the reported aging rate constant of S_P-cycloheptyl methyl conjugated wild-type AChE (0.0004 min^{-1}; *18*).

In a previous study it was shown that spontaneous reactivation of phosphonylated *Torpedo californica* AChE and human plasma BChE by cycloheptyl, isopropyl, and 3,3-dimethylbutyl methylphosphonyl thiocholine enantiomers

Table 1: Reactivation of Recombinant DNA-Derived Mouse Cholinesterases Phosphonylated with S_P-Cycloheptyl Methylphosphonyl Thiocholine[a]

reactivator (mM)	enzyme	k_{+2} (min^{-1})	K_{ox} (mM)	k_r ($min^{-1} M^{-1}$)	% $react_{max}$	time
HI-6 (0.2−20)	AChE wt	0.60 ± 0.04	5.4 ± 0.8	112 ± 19	90	5 min
HI-6 (0.02−0.5)	Y337A			2000 ± 90	80	1 min
HI-6 (0.002−0.1)	F295L/Y337A			13180 ± 1414	80	3 min
HI-6 (0.01−5)	F297I/Y337A	6.0 ± 0.5	2.6 ± 0.4	2300 ± 400	100	1 min
HI-6 (0.2−10)	Y337A/F338A	0.051 ± 0.003	0.50 ± 0.12	102 ± 26	80	30 min
HI-6 (10)	F295L/F297I/Y337A[b]			≥24	80	20 min
HI-6 (1, 30)	BChE wt				<10	48 h
2-PAM (1−20)	AChE wt	0.0040 ± 0.0007	6.1 ± 3.0	0.66 ± 0.34	70	15 h
2-PAM (0.1−40)	Y337A	0.0025 ± 0.0001	0.62 ± 0.14	4.1 ± 1.0	80	5 h
2-PAM (0.4−20)	F295L/Y337A	0.016 ± 0.003	10 ± 3	1.7 ± 0.5	70	3 h
2-PAM (2−30)	F297I/Y337A	0.018 ± 0.002	2.7 ± 1.2	6.9 ± 3.3	70	2 h
2-PAM (1−60)	Y337A/F338A	0.00035 ± 0.00002	0.75 ± 0.45	0.47 ± 0.29	40	25 h
2-PAM (40)	F295L/F297I/Y337A[b]			≥0.12	100	5 h
2-PAM (5, 40)	BChE wt				<5	48 h

[a] Constants (±standard errors) are calculated (eqs 1−3) from k_{obs} constants (8−16 values) obtained in two to seven experiments. The maximal percent of reactivation (% $react_{max}$) measured within the specified time of the experiment is also given. [b] Only one k_{obs} was determined (0.24 ± 0.04 min^{-1} with HI-6 and 0.0048 ± 0.0011 min^{-1} with 2-PAM).

Table 2: Reactivation of Recombinant DNA-Derived Mouse Cholinesterases Phosphonylated with S_P-3,3-Dimethylbutyl Methylphosphonyl Thiocholine[a]

reactivator (mM)	enzyme	k_{+2} (min^{-1})	K_{ox} (mM)	k_r ($min^{-1} M^{-1}$)	% $react_{max}$	time
HI-6 (0.05−5)	AChE wt	0.39 ± 0.09	3.8 ± 1.8	102 ± 53	80	10 min
HI-6 (0.05−5)	Y337A	3.2 ± 0.5	2.8 ± 1.0	1200 ± 490	100	2 min
HI-6 (0.01−1)	F295L/Y337A			1300 ± 60	100	2 min
HI-6 (0.01−10)	F297I/Y337A	1.4 ± 0.1	1.9 ± 0.5	720 ± 180	100	5 min
HI-6 (1−40)	Y337A/F338A	0.10 ± 0.01	2.1 ± 1.2	47 ± 28	80	20 min
HI-6 (10)	F295L/F297I/Y337A[b]			≥31	80	10 min
HI-6 (0.5−20)	BChE wt	0.73 ± 0.14	7.1 ± 3.2	103 ± 51	100	10 min
2-PAM (1−40)	AChE wt			0.18 ± 0.01	90	8 h
2-PAM (5−40)	Y337A			0.041 ± 0.003	80	33 h
2-PAM (0.5−40)	F295L/Y337A	0.0018 ± 0.0002	2.8 ± 1.1	0.66 ± 0.27	90	25 h
2-PAM (10−60)	F297I/Y337A	0.0025 ± 0.0002	9.0 ± 3.6	0.27 ± 0.11	80	15 h
2-PAM (5−60)	Y337A/F338A	0.00023 ± 0.00001	0.54 ± 0.85	0.42 ± 0.65	60	70 h
2-PAM (40)	F295L/F297I/Y337A[b]			≥0.22	90	6 h
2-PAM (3−30)	BChE wt	0.028 ± 0.003	3.2 ± 1.7	8.7 ± 4.6	100	3 h

[a] Constants (±standard errors) are calculated (eqs 1−3) from k_{obs} constants (5−15 values) obtained in two to four experiments. The maximal percent of reactivation (% $react_{max}$) measured within the specified time of the experiment is also given. [b] Only one k_{obs} was determined (0.31 ± 0.06 min^{-1} with HI-6 and 0.0088 ± 0.0021 min^{-1} with 2-PAM).

Table 3: Reactivation of Recombinant DNA-Derived Mouse Cholinesterases Phosphonylated with S_P-Isopropyl Methylphosphonyl Thiocholine[a]

reactivator (mM)	enzyme	k_{+2} (min^{-1})	K_{ox} (mM)	k_r ($min^{-1} M^{-1}$)	% $react_{max}$	time (min)
HI-6 (0.05−1)	AChE wt	0.20 ± 0.03	0.15 ± 0.09	1330 ± 780	90	10
HI-6 (0.2−20)	Y337A	1.13 ± 0.08	4.7 ± 0.8	240 ± 47	100	2
HI-6 (0.5−30)	F295L/Y337A	0.27 ± 0.01	0.37 ± 0.09	730 ± 180	80	10
HI-6 (0.05−1)	F297I/Y337A	0.95 ± 0.13	0.41 ± 0.14	2330 ± 844	100	5
HI-6 (1−20)	Y337A/F338A	0.26 ± 0.02	1.5 ± 0.6	178 ± 74	90	15
HI-6 (0.05−5)	BChE wt	0.014 ± 0.001	0.064 ± 0.024	215 ± 70	80	90
2-PAM (0.1−10)	AChE wt	0.095 ± 0.013	0.088 ± 0.075	1080 ± 940	100	30
2-PAM (0.2−40)	Y337A	0.21 ± 0.01	2.6 ± 0.3	82 ± 11	80	20
2-PAM (1−40)	F295L/Y337A			3.5 ± 0.4	90	30
2-PAM (0.1−40)	F297I/Y337A	2.9 ± 0.2	5.5 ± 1.3	534 ± 133	90	1
2-PAM (1−40)	Y337A/F338A	0.072 ± 0.004	1.5 ± 0.5	46 ± 14	90	30
2-PAM (0.05−10)	BChE wt	2.98 ± 0.01	2.39 ± 0.02	1250 ± 9	90	1

[a] Constants (±standard errors) are calculated (eqs 1−3) from k_{obs} constants (6−19 values) obtained in two to five experiments. The maximal percent of reactivation (% $react_{max}$) measured within the specified time of the experiment is also given.

proceeded very slowly, if at all (rate constants less than 0.001 min^{-1}) (*23*). In initial studies, we did not observe spontaneous reactivation with return of AChE activity in several of the methylphosphonyl conjugates studied as we have observed for the dimethyl, diethyl, and diisopropylphosphoryl conjugates of mouse AChE (*24*). The phosphonyl oxime (product of reactivation) could reinhibit the free enzyme (*2*, *25*, *26*), but we have yet to identify the inhibitory potency and the stability of these reactivation products.

Oxime Reactivation of the S_P-Alkyl Methylphosphonylated Cholinesterases. The kinetic parameters for reactivation of the S_P-cycloheptyl, S_P-3,3-dimethylbutyl, and S_P-isopropyl methylphosphonylated cholinesterases by HI-6 and 2-PAM are presented in Tables 1−3. All S_P conjugates were

Table 4: Reactivation of Recombinant DNA-Derived Mouse Cholinesterases Phosphonylated with R_P-Cycloheptyl Methylphosphonyl Thiocholine[a]

reactivator (mM)	enzyme	k_{+2} (min^{-1})	K_{ox} (mM)	k_r ($min^{-1} M^{-1}$)	% $react_{max}$	time (h)
HI-6 (1, 40)	AChE wt				<15	50
HI-6 (0.3−20)	Y337A	0.00042 ± 0.00002	1.0 ± 0.2	0.41 ± 0.06	50	85
HI-6 (1−30)	F295L/Y337A				<25	40
HI-6 (10−40)	F297I/Y337A				<25	72
HI-6 (0.2−2)	Y337A/F338A				<15	40
HI-6 (10−30)	BChE wt				<15	50
2-PAM (1, 40)	AChE wt				<25	50
2-PAM (0.3−5)	Y337A	0.00047 ± 0.00004	0.36 ± 0.16	1.3 ± 0.6	50	85
2-PAM (20−40)	F295L/Y337A				<25	40
2-PAM (5−40)	F297I/Y337A				<40	60
2-PAM (0.3−5)	Y337A/F338A	0.00040 ± 0.00010	0.99 ± 0.87	0.40 ± 0.37	40	20
2-PAM (20−40)	BChE wt			0.027 ± 0.001	70	25

[a] Constants (±standard errors) are calculated (eqs 1−3) from k_{obs} constants (4−8 values) obtained in one to three experiments. The maximal percent of reactivation (% $react_{max}$) measured within the specified time of the experiment is also given.

Table 5: Reactivation of Recombinant DNA-Derived Mouse Cholinesterases Phosphonylated with R_P-3,3-Dimethylbutyl Methylphosphonyl Thiocholine[a]

reactivator (mM)	enzyme	k_{+2} (min^{-1})	K_{ox} (mM)	k_r ($min^{-1} M^{-1}$)	% $react_{max}$	time (h)
HI-6 (0.2−2)	AChE wt				<15	40
HI-6 (0.2−40)	Y337A	0.00040 ± 0.00002	0.54 ± 0.14	0.74 ± 0.19	70	35
HI-6 (1,10)	F295L/Y337A				<25	60
HI-6 (10−40)	F297I/Y337A				<25	60
HI-6 (0.2−2)	Y337A/F338A	0.00014 ± 0.00001	0.076 ± 0.051	1.8 ± 1.2	50	40
HI-6 (1−10)	BChE wt				<25	50
2-PAM (0.3−5)	AChE wt				<15	40
2-PAM (0.5−5)	Y337A	0.0007 ± 0.0000	0.38 ± 0.08	1.8 ± 0.4	60	35
2-PAM (5, 30)	F295L/Y337A				<25	60
2-PAM (20−60)	F297I/Y337A				<25	60
2-PAM (0.3−5)	Y337A/F338A				<15	60
2-PAM (3−30)	BChE wt	0.0079 ± 0.0011	13 ± 4	0.62 ± 0.22	80	20

[a] Constants (±standard errors) are calculated (eqs 1−3) from k_{obs} constants (4−8 values) obtained in one or two experiments. The maximal percent of reactivation (% $react_{max}$) measured within the specified time of the experiment is also given.

Table 6: Reactivation of Recombinant DNA-Derived Mouse Cholinesterases Phosphonylated with R_P-Isopropyl Methylphosphonyl Thiocholine[a]

reactivator (mM)	enzyme	k_{+2} (min^{-1})	K_{ox} (mM)	k_r ($min^{-1} M^{-1}$)	% $react_{max}$	time (h)
HI-6 (0.2−40)	AChE wt	0.0075 ± 0.0003	4.3 ± 0.7	1.7 ± 0.3	70	10
HI-6 (0.2−30)	Y337A	0.0071 ± 0.0004	0.97 ± 0.23	7.3 ± 1.8	80	8
HI-6 (1−30)	F295L/Y337A	0.0013 ± 0.0001	0.95 ± 0.56	1.3 ± 0.8	70	16
HI-6 (5−40)	F297I/Y337A	0.0021 ± 0.0003	16 ± 8	0.13 ± 0.07	50	16
HI-6 (1−30)	BChE wt	0.00035 ± 0.00004	1.1 ± 0.9	0.23 ± 0.25	40	25
2-PAM (0.3−40)	AChE wt	0.0029 ± 0.0004	1.9 ± 1.1	1.5 ± 0.9	70	20
2-PAM (0.3−40)	Y337A	0.0026 ± 0.0001	0.60 ± 0.21	4.3 ± 1.5	80	8
2-PAM (5−30)	F295L/Y337A	0.0096 ± 0.0039	10 ± 11	0.95 ± 1.09	80	10
2-PAM (5−60)	F297I/Y337A			0.041 ± 0.003	100	25
2-PAM (5−30)	BChE wt	0.024 ± 0.006	27 ± 13	0.88 ± 0.47	100	4

[a] Constants (±standard errors) are calculated (eqs 1−3) from k_{obs} constants (6−10 values) obtained in two to four experiments. The maximal percent of reactivation (% $react_{max}$) measured within the specified time of the experiment is also given.

reactivated nearly completely with the exception of S_P-cycloheptyl methylphosphonylated BChE (cf. Table 1). The S_P-cycloheptyl methylphosphonylated F295L/F297I/Y337A mutant, structurally the most similar to BChE in substituted active center gorge residues, was reactivated between 80% and 100% by both oximes.

Reactivation of all S_P-phosphonylated AChE and mutant conjugates by HI-6 was appreciably faster than by 2-PAM. The difference in k_r between oximes is primarily dictated by the unimolecular reaction step, k_{+2}, which is more than 100-fold slower for 2-PAM than HI-6. Single or double substitutions involving F295L, F297I, and Y337A within the AChE gorge enhanced the k_r in reactivation of mutants phosphonylated with bulky methylphosphonates (cycloheptyl and 3,3-dimethylbutyl; Tables 1 and 2), while only the F297I/Y337A double mutation enhanced reactivation of all three S_P conjugates. The greatest enhancement of k_r (about 120-fold) over the wild-type AChE was obtained in reactivation of S_P-cycloheptyl methylphosphonyl F295L/Y337A AChE by HI-6 (cf. Table 1); the determined k_r was the greatest for all reactions reported in this paper.

Both wild-type AChE and BChE phosphonylated with S_P-isopropyl methylphosphonate were reactivated by both oximes more rapidly (higher k_r value) than the wild-type enzymes phosphonylated by the more bulky S_P-3,3-dimethylbutyl and S_P-cycloheptyl methylphosphonates (cf. Table 3 vs Tables 1 and 2). Although k_r for 2-PAM reactivation of wild-type AChE and BChE was similar, the component K_{ox}

and k_{+2} constants differed by 30-fold where phosphonylated AChE had a higher affinity (i.e., lower K_{ox}) and lower k_{+2} for 2-PAM, and on the other hand, phosphonylated BChE had a higher maximum reactivation rate constant (k_{+2}).

Oxime Reactivation of the R_P-Alkyl Methylphosphonylated Cholinesterases. Tables 4−6 present results for reactivation of the R_P-cycloheptyl, R_P-3,3-dimethylbutyl, and R_P-isopropyl methylphosphonylated enzymes. HI-6 and 2-PAM showed similar but low reactivation efficiency (from 34 conjugates only 18 were reactivated). For the bulky R_P-cycloheptyl (Table 4) and R_P-3,3-dimethylbutyl (Table 5) methylphosphonylated wild-type AChE reactivation was not evident with either HI-6 or 2-PAM, while the corresponding BChE conjugates were reactivated by 2-PAM nearly completely albeit at slow rates. Hence, 2-PAM reactivation showed an inverted stereoselectivity for the cycloheptyl methylphosphonyl BChE conjugate: the S_P conjugate was resistant to reactivation (cf. Table 1), while the R_P conjugate was reactivated.

Reactivation kinetics of mouse single residue mutants of AChE conjugated with these methylphosphonates was previously studied by Wong et al. (*18*). Data given in the present paper agree with the reported results except for the reactivation of wild-type AChE conjugated with R_P-3,3-dimethylbutyl methylphosphonate (Table 5). In the present experiments this conjugate was found not to be reactivatable, while in previous experiments substantial reactivation was observed by both oximes (*18*). In the previous study inhibition was carried out at a 14-fold excess of organophosphate, on average (range of 4-fold to 22-fold), and inhibition by a minor abundance of the S_P contaminant may have predominated under this condition. This situation was avoided in the current studies by using inhibitors in only 10% stoichiometric excess.

Reactivation rates of the less bulky R_P-isopropyl methyl phosphonylated enzymes presented in Table 6 were generally more rapid than the conjugates phosphonylated with the larger two R_P-phosphonates. The highest bimolecular reactivation rate for the R_P conjugate of Y337A was 7.3 min^{-1} M^{-1} for HI-6 and 4.3 min^{-1} M^{-1} for 2-PAM. Comparing these reactivation rates with the rates of R_P-Y337A conjugates in Tables 4 and 6, it follows that R_P-isopropyl methyl phosphonylated Y337A had the highest k_{+2} value. The Y337A mutation coupled with F338A also showed appreciable rates of reactivation of R_P-cycloheptyl methylphosphonyl Y337A/F338A AChE by 2-PAM and R_P-3,3-dimethylbutyl methylphosphonyl Y337A/F338A AChE by HI-6, but reactivation was not complete.

Molecular Modeling. Models of the reversible Michaelis-type complexes (Figure 3; [EP][OX] in Scheme 1) between HI-6 and either S_P-cycloheptyl methylphosphonylated wild-type mouse AChE or F295L/Y337A mouse AChE resulting from molecular dynamics calculation indicate that, with the wild-type enzyme, HI-6 can assume only one distinct productive orientation with the slender molecule extended through the narrow gorge (Figure 3B). Within the enlarged gorge of the F295L/Y337A mutant AChE additional orientations appear likely. The HI-6 chain coils back into the enlarged choline binding site where the nonreactive carbamoyl pyridinium moiety is stabilized (cf. Figure 3A,C). The distance between the oxime oxygen and the phosphorus in wild-type conformations (4.2 ± 1.0 Å, $n = 20$) and mutant gorge conformations (4.5 ± 0.9 Å, $n = 20$) appeared very similar and consistent with distances found for similar oxime−AChE complex models obtained by other authors (about 4.4 Å measured for the structure deposited by Pang et al.: PDB accession codes 1JGA and 1JGB; *27*).

DISCUSSION

Reactivation by the two oximes demonstrates the superiority of HI-6 over 2-PAM for reactivation of wild-type AChE and mutant S_P-phosphonate conjugates. Moreover, the enzyme conjugates showed a high degree of stereoselectivity for HI-6 reactivation, with preference of S_P over R_P enantiomers. Taken together with previous findings on organophosphate inactivation (*9*, *10*, *13*) and reactivation (*18*, *25*, *28*), oxime-mediated reactivation is governed by several principles.

Similar to inhibition by phosphonates, reactivation efficiency is enhanced by phosphonyl oxygen insertion into the oxyanion hole in the presumed transition state. Owing to the spatial constraints of the acyl pocket, the bulky R_P-methylphosphonates cannot achieve optimal positioning of alkoxy groups without distortion of structure. Accordingly, just as the R_P inhibitors react far more slowly with AChE (*9*, *10*, *13*), they are either resistant to reactivation or reactivate slowly (*18*). For R_P conjugates suboptimal positioning of the phosphonyl oxygen in the oxyanion hole and limitations on oxime access to the phosphonate both slow reactivation rates. However, a single mutation of the choline binding site, Y337A, enabled reactivation of the R_P conjugates. Reactivation was increased presumably because of an improved clearance in the formation of the pentacoordinate transition state and the reduction in steric constraints around residue 337. The tetrahedral phosphonate may move slightly toward the vacant area created by removal of the aromatic side chain at position 337, allowing a more favorable angle of oxime attack.

The spatial constraints of the gorge give rise to a dimensionally impacted organophosphate with a limited angle of access for the attacking nucleophile. Our previous studies of acyl pocket mutations suggest a nucleophilic attack route to the phosphorus atom coming from the acyl pocket direction (*18*). We show in this paper that enhancing clearance in the vicinity of Y337 has an influence on reactivation rates. Indeed, the double mutation involving F295 and Y337 yields the greatest rate enhancement. This suggests that the route of oxime attack still occurs from the acyl pocket side, but the tethered phosphonate is able to adopt an exposed position more amenable to attack, or new orientations of the attacking oxime allowed by the vacant area created near residue 337 optimize the attack angle.

The likely position of HI-6 in the mutant F295L/Y337A for the attack on phosphonylated serine is shown in Figure 3A. Simply opening the AChE choline binding site in all dimensions to enhance access of the oxime group to the phosphorus atom is not sufficient to increase reactivation. Additional substitution by F338A leading to a more open gorge appeared counterproductive for reactivation (cf. Table 1). Certain aromatic residues may be required in order to stabilize the oxime in the proper orientation between F338 and F297 as shown in Figure 3. Hence, reactivation of S_P-cycloheptyl methylphosphonyl Y337A/F338A conjugate was

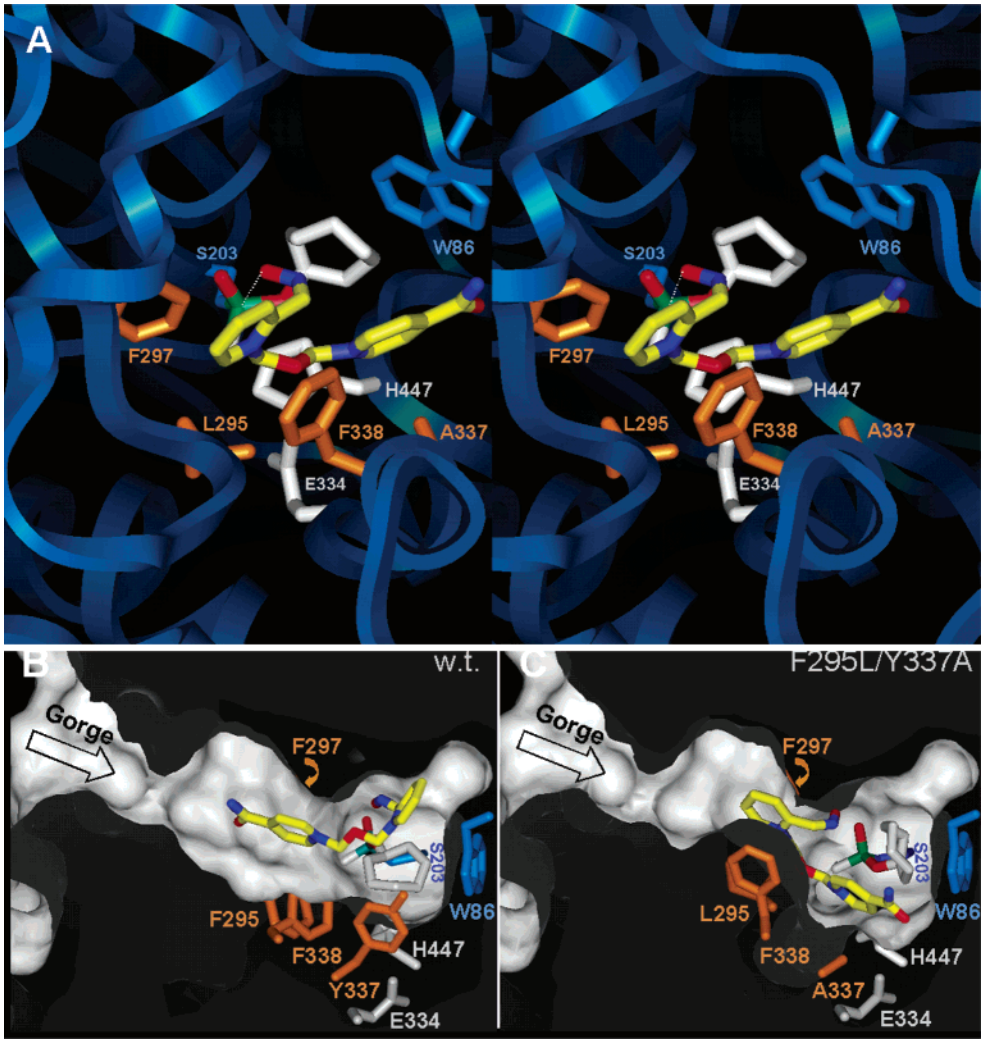

FIGURE 3: (A) Stereo image of an energy-minimized HI-6 conformation (carbon atoms in yellow, nitrogen in blue, oxygen in red) in the F295L/Y337A mouse AChE (in blue ribbon) S_P-cycloheptyl methylphosphonylated active center gorge. The active center is viewed through the gorge opening. The lowest energy conformer is shown, out of a cluster of 20 similar resulting conformations. The dotted white line indicates the direction of nucleophilic attack of HI-6. Only selected AChE residues are displayed in blue, white (catalytic triad), and orange (residues mutated in this study). (B, C) Cutaway diagrams at identical angles of the HI-6 complex with wild-type mouse AChE (panel B) and in the F295L/Y337A mutant mouse AChE (panel C). The AChE represented by Connolly solvent-accessible surface was cut approximately in half to reveal the position, size, and depth of the active center gorge in the wild-type and mutant AChE. The orange arrow indicates the position of the F297 side chain hidden behind a surface.

not as efficient as was reactivation of the F295L/Y337A conjugate.

While opening of the gorge can greatly enhance oxime efficacy, a gorge devoid of critical aromatic residues or a tethered phosphonate with many degrees of freedom and torsional movement, as found for BChE, yields an environment not conducive to efficient reactivation by HI-6, whereas reactivation by the smaller, but less efficient, 2-PAM molecule is less influenced by this difference. Hence, efficacy of oximes is dependent not only on the oxime structure but also on the position of the conjugated phosphorus residue. Attack by the oxime is believed to proceed through a pentavalent (trigonal bipyramidyl) intermediate and formation of the phosphorylated oxime. Both 2-PAM and HI-6 have their oxime groups in the *ortho* position to the cationic pyridinium nitrogen, and their attacking orientations should have distinctive steric constraints. Hence, the inability of 2-PAM and HI-6 to cause reactivation of certain conjugates, particularly R_P conjugates, may not prevail for all oximes. Obidoxime and TMB-4, two symmetric dioximes with oxime groups *para* to the pyridinium ring, reactivate R_P conjugates to near completion although at very slow rates (*18*, *23*). Fortunately, the R_P enantiomers that are resistant to oxime reactivation are also less reactive as phosphonylation agents (*9*, *10*, *13*). Hence, they will be the less reactive and toxic of the chiral pair.

A practical outgrowth of these studies is the application of mutant AChE−oxime combinations to catalyze the hydrolysis of organophosphates both in vitro and in vivo. Cholinesterases in the plasma are efficient scavengers of organophosphates in terms of reactivity; however, their capacity is limited by virtue of the 1:1 stoichiometry between the small organophosphate (100−200 Da) and the ~70 kDa subunit bearing the catalytic serine. Hence, an enzyme−reactivator combination catalytic to the organophosphate hydrolysis, rather than stoichiometric to conjugation, would greatly reduce doses needed for scavenging.

Lockridge et al. (*17*) generated mutations in butyrylcholinesterase that catalyze the hydrolysis of organophosphates. However, mutations that enable organophosphate turnover

also compromise its capacity to react initially with the organophosphate, thus limiting the potential of butyrylcholinesterase in vivo. By contrast, the mutations described here that enhance oxime reactivation react efficiently with the methylphosphonates as described previously (*13*), and the limitations in scavenging capacity then depend on efficiency of the oxime to continually regenerate active AChE. By enhancing the rate some 120-fold, we approach a range where scavenging efficiency has a practical outcome. Efficiency of scavenging is also a pharmacokinetic consideration since the introduced organophosphate must be scavenged in the plasma before it distributes into extracellular space and/or accesses the blood−brain barrier. As shown here, the enhanced scavenging capacity is manifested to the greatest extent in those bulky S_P enantiomers that are most intractable to reactivation. Of the offending methylphosphonates, cyclosarin and soman would fall into this category.

REFERENCES

1. Chambers, H. W. (1992) Organophosphorus compounds: An Overview, in *Organophosphates: Chemistry, Fate, and Metabolism* (Chambers, J. E., and Levi, P. E., Eds.) pp 3−17, Academic Press, San Diego, CA.
2. Wilson, I. B., and Ginsburg, S. (1955) A powerful reactivator of alkylphosphate-inhibited acetylcholinesterase, *Biochim. Biophys. Acta 18*, 168−170.
3. Froede, H. C., and Wilson, I. B. (1971) Acetylcholinesterase, in *The Enzymes* (Boyer, P. D., Ed.) 3rd ed., Vol. 5, pp 87−114, Academic Press, New York and London.
4. Flanagan, J., and Jones, A. L. (2001) *Antidotes*, pp 245−267, Taylor and Francis, London and New York.
5. Sussman, J. L., Harel, M., Frolow, F., Oefner, C., Goldman, A., Toker, L., and Silman, I. (1991) Atomic structure of acetylcholinesterase from *Torpedo californica*: A prototypic acetylcholine-binding protein, *Science 253*, 872−897.
6. Bourne, Y., Taylor, P., and Marchot, P. (1995) Acetylcholinesterase inhibition by fasciculin: crystal structure of the complex, *Cell 83*, 503−512.
7. Kryger, G., Harel, M., Giles, K., Toker, L., Velan, B., Lazar, A., Kronman, C., Barak, D., Ariel, N., Shafferman, A., Silman, I., and Sussman, J. L. (2000) Three-dimensional structure of a complex of E2020 with acetylcholinesterase from *Torpedo californica*, *Acta Crystallogr., Sect. D 56*, 1385−1394.
8. Berman, H. A., and Leonard, K. (1989) Chiral reactions of acetylcholinesterase probed with enantiomeric methylphosphonothioates, *J. Biol. Chem. 264*, 3942−3950.
9. Hosea, N. A., Berman, H. A., and Taylor, P. (1995) Specificity and orientation of trigonal carboxylesters and tetrahedral phosphonylesters in cholinesterase, *Biochemistry 34*, 11528−11536.
10. Hosea, N. A., Radić, Z., Tsigelny, I., Berman, H. A., Quinn, D. M., and Taylor, P. (1996) Aspartate 74 as a primary determinant in acetylcholinesterase governing specificity to cationic organophosphates, *Biochemistry 35*, 10995−11004.
11. Taylor, P., Hosea, N. A., Tsigelny, I., Radić, Z., and Berman, H. A. (1997) Determining ligand orientation and transphosphonylation mechanism on acetylcholinesterase by R_P, S_P enantiomer selectivity and site-specific mutagenesis, *Enantiomer 2*, 249−260.
12. Ordentlich, A., Barak, D., Kronman, C., Benschop, H. P., De Jong, L. P. A., Ariel, N., Barak, R., Segall, Y., Velan, B., and Shafferman, A. (1999) Dissection of the human acetylcholinesterase active center determinants of substrate specificity—Identification of residues constituting the anionic site, the hydrophobic site, and the acyl pocket, *Biochemistry 38*, 3055−3066.
13. Kovarik, Z., Radić, Z., Berman, H. A., Simeon-Rudolf, V., Reiner, E., and Taylor, P. (2003) Acetylcholinesterase active centre and gorge conformations analysed by combinatorial mutations and enantiomeric phosphonates, *Biochem. J. 373*, 33−40.
14. Ashani, Y., Radić, Z., Tsigelny, I., Vellom, D. C., Pickering, N., Quinn, D. M., Doctor, B. P., and Taylor, P. (1995) Amino acid residues controlling reactivation of organophosphonyl conjugates of acetylcholinestrase by mono- and bisquaternary oximes, *J. Biol. Chem. 270*, 6370−6380.
15. Grosfeld, H., Barak, D., Ordentlich, A., Velan, B., and Shafferman, A. (1996) Interactions of oxime reactivators with diethylphosphoryl adducts of human acetylcholinesterase and its mutant derivatives, *Mol. Phamacol. 50*, 639−649.
16. Masson, P., Froment, M.-T., Bartels, C. F., and Lockridge, O. (1997) Importance of aspartate-70 in organophosphate inhibition, oxime re-activation and aging of human butyrylcholinesterase, *Biochem. J. 325*, 53−61.
17. Lockridge, O., Blong, R. M., Masson, P., Froment, M.-T., Millard, C. B., and Broomfield, C. A. (1997) A single amino acid substitution, Gly117His, confers phosphotriesterase (organophosphorus acid anhydride hydrolase) activity on human butyrylcholinesterase, *Biochemistry 36*, 786−795.
18. Wong, L., Radić, Z., Brüggemann, R. J. M., Hosea, N., Berman, H. A., and Taylor, P. (2000) Mechanism of oxime reactivation of acetylcholinesterase analyzed by chirality and mutagenesis, *Biochemistry 39*, 5750−5757.
19. Radić, Z., Pickering, N. A., Vellom, D. C., Camp, S., and Taylor, P. (1993) Three distinct domains in the cholinesterase molecule confer selectivity for acetylcholinesterase and butyrylcholinesterase inhibitors, *Biochemistry 32*, 12074−12084.
20. Ordentlich, A., Barak, D., Kronman, C., Flashner, Y., Leitner, M., Segall, Y., Ariel, N., Cohen, S., Velan, B., and Shafferman, A. (1993) Dissection of the human acetylcholinesterase active center determinants of substrate specificity—Identification of residues constituting the anionic site, the hydrophobic site, and the acyl pocket, *J. Biol. Chem. 268*, 17083−17095.
21. Marchot, P., Ravelli, R. B. G., Raves, M. L., Bourne, Y., Vellom, D. C., Kanter, J., Camp, S., Sussman, J. L., and Taylor, P. (1996) Soluble monomeric acetylcholinesterase from mouse—expression, purification, and crystallization in complex with fasciculin, *Protein Sci. 5*, 672−679.
22. Ellman, G. L., Courtney, K. D., Andres, V., Jr., and Featherstone, R. M. (1961) A new and rapid colorimetric determination of acetylcholinesterase activity, *Biochem. Pharmacol. 7*, 88−95.
23. Berman, H. A. (1998) A view from the gorge. Reactivation and importance of water, in *Structure and Function of Cholinesterases and Related Proteins* (Doctor, B. P., Taylor, P., Quinn, D. M., Rotundo, R. L., and Gentry, M. K., Eds.) pp 413−417, Plenum Press, New York and London.
24. Jennings, L. L., Malecki, M., Komives, E. A., and Taylor, P. (2003) Direct analysis of the kinetic profiles of organophosphate-acetylcholinesterase adducts by MALDI-TOF mass spectrometry, *Biochemistry 42*, 11083−11091.
25. Luo, C., Saxena, A., Smith, M., Garcia, G., Radić, Z., Taylor, P., and Doctor, B. P. (1999) Phosphoryl oxime inhibition of acetylcholinesterase during oxime reactivation is prevented by edrophonium, *Biochemistry 38*, 9937−9947.
26. Ashani, Y., Bhattacharjee, A. K., Leader, H., Saxena, A., and Doctor, B. P. (2003) Inhibition of cholinesterase with cationic phosphonyl oximes highlights distinctive properties of the charged pyridine groups of quaternary oxime reactivators, *Biochem. Pharmacol. 33*, 191−202.
27. Pang, Y.-P., Kollmeyer, T. M., Hong, F., Lee, J.-C., Hammond, P. I., Haugabouk, S. P., and Brimijoin, S. (2003) Rational design of alkylene-linked bis-pyridiniumaldoximes as improved acetylcholinesterase reactivators, *Chem. Biol. 10*, 491−502.
28. Luo, C., Leader, H., Radic, Z., Maxwell, D. M., Taylor, P., Doctor, B. P., and Saxena, A. (2003) Two possible orientations of the HI-6 molecule in the reactivation of organophosphate-inhibited acetylcholinesterase, *Biochem. Pharmacol. 66*, 387−392.

BI036191A